Published in final edited form as:
Cell. 2009 September 18; 138(6): 1209–1221. doi:10.1016/j.cell.2009.06.042.

The antioxidant enzyme Prdx1 controls neuronal differentiation by thiol-redox dependent activation of GDE2

Ye Yan[1], **Priyanka Sabharwal**[1], **Meenakshi Rao**[1,2], and **Shanthini Sockanathan**[1,*]

[1] The Solomon H. Snyder Department of Neuroscience, Johns Hopkins University School of Medicine, 725 N. Wolfe Street, Baltimore, MD 21205, USA. ssockan1@jhmi.edu, Phone: (410) 502-3084; Fax: (410) 614-8423

Summary

The six-transmembrane protein GDE2 comprises a new signaling system that controls the onset and progression of spinal motor neuron differentiation through extracellular glycerophosphodiester phosphodiesterase metabolism. However, the mechanisms that regulate its activity are unknown. Here we show that the antioxidant scavenger Peroxiredoxin1 (Prdx1) interacts with GDE2, and that loss of Prdx1 causes motor neuron deficits analogous to GDE2 ablation. Prdx1 cooperates with GDE2 to drive motor neuron differentiation, and this synergy requires Prdx1 thiol-dependent catalysis. Prdx1 activates GDE2 through reduction of an intramolecular disulfide bond bridging its intracellular N- and C-terminal domains that normally gates GDE2 activity. GDE2 variants incapable of disulfide bond formation acquire independence from Prdx1, and are potent inducers of motor neuron differentiation. These findings define Prdx1 as a pivotal regulator of GDE2 activity, and reveal critical roles for coupled thiol redox-dependent cascades in controlling neuronal differentiation in the spinal cord.

Introduction

The assembly of functional neural circuits depends upon the precisely controlled temporal and spatial differentiation of distinct neuronal subtypes (Jessell, 2000; Kintner, 2002). Deregulated differentiation can lead to severe deficits including the depletion of progenitor pools, imbalances in neuronal diversity and number, and at the other extreme, unchecked proliferation and tumor formation (Bertram, 2000; Kintner, 2002). While the transcriptional pathways that control the transition between proliferation and differentiation are emerging, the regulatory mechanisms that control this switch are poorly understood (Jessell, 2000).

The differentiation of spinal motor neurons has proved to be a useful paradigm to understand the molecular mechanisms that control neuronal differentiation (Jessell, 2000). Retinoic acid (RA) signals trigger the differentiation of motor neuron progenitors into postmitotic motor neurons in part by downregulating Olig2, which maintains cells in a motor neuron progenitor state (Mizuguchi et al., 2001; Novitch et al., 2001; Novitch et al., 2003; Lee et al., 2005). Decreased Olig2 expression causes a change in the equilibrium of Olig2 and the proneural protein Ngn2, causing the parallel implementation of neurogenic and motor neuron fate

*Correspondence and requests for material should be addressed to S.S. (ssockan1@jhmi.edu).
[2]present address: Department of Medicine, Children's Hospital Boston

specification programs (Lee et al., 2005). These events correlate with changes in cell-body position along the medial-lateral axis of the spinal cord that accurately reflect the progress of motor neuron differentiation (Jessell, 2000; Hollyday, 2001). Thus, actively cycling $Olig2^+$ motor neuron progenitors reside within the ventricular zone (VZ), but after completing their terminal mitosis at the medial margin of the VZ, $Olig2^+$ progenitors undergo cell cycle arrest and migrate laterally into the intermediate zone (IZ) (Figure S1; Hollyday, 2001). Subsequently, differentiating cells in the IZ downregulate progenitor markers, express postmitotic motor neuron markers such as Islet1 and HB9, and migrate laterally to occupy their final settling positions in the ventral horn (Figure S1; Jessell, 2000; Hollyday, 2001).

The molecular pathways that link RA signaling pathways to the transcriptional programs that regulate the transition from proliferation to differentiation are beginning to emerge. RA signaling triggers motor neuron differentiation by upregulating GDE2, a six transmembrane protein containing an extracellular glycerophosphodiester phosphodiesterase (GDPD) domain. GDE2 is necessary and sufficient to drive motor neuron differentiation by coordinately triggering neurogenic and motor neuron fate specification pathways (Nogusa et al., 2004; Rao and Sockanathan, 2005; Yanaka et al., 2007). Single point mutations that negate GDE2 GDPD function fail to induce motor neuron differentiation, revealing GDE2 as an unprecedented signaling system that drives motor neuron differentiation through extracellular GDPD activity (Zheng et al., 2003; Santelli et al., 2004; Rao and Sockanathan, 2005). GDE2 belongs to a vertebrate-specific family of six-transmembrane GDPD containing proteins that includes GDE3 and GDE6 (Nogusa et al., 2004; Yanaka et al., 2003; Yanaka, 2007). GDE3 is capable of driving osteoblast differentiation in vitro, suggesting that these proteins are a unique family of signaling molecules that critically regulate differentiation in diverse cellular contexts (Yanaka et al., 2003; Yanaka, 2007).

Loss of GDE2 leads to deficits in motor neuron production, whereas premature exposure of progenitors to GDE2 GDPD signals precipitates differentiation and the depletion of progenitors (Rao and Sockanathan, 2005). Thus, the precise regulation of GDE2 activity is a critical prerequisite for the normal progression of spinal motor neuron differentiation. However, virtually nothing is known of the mechanisms that control GDE2 function, and how it integrates with cellular regulatory networks. In order to define the mechanisms that regulate GDE2 function, we carried out unbiased proteomic screens to isolate proteins that interact with GDE2. Here, we identify the antioxidant enzyme Prdx1 as an interactor of GDE2 and uncover a novel developmental role for Prdx1 in regulating neuronal differentiation in the spinal cord. Prdx1 is a 2-Cysteine (Cys) thiol reductase that forms a component of cellular antioxidant and thermal stress defense mechanisms through its ability to metabolize H_20_2, and its properties as a molecular chaperone (Wood et al., 2003; Rhee et al., 2005; Jang et al., 2004). We show here that Prdx1 is expressed in differentiating progenitors in the developing spinal cord. Ablation of Prdx1 causes deficits in motor neuron differentiation but no changes in the specification or number of $Olig2^+$ progenitors, reminiscent of GDE2 loss of function phenotypes. Prdx1 binds and activates GDE2 by causing the reduction of an intramolecular disulfide bond between the N- and C-terminal domains of GDE2 that normally gates its function. Single point mutants of GDE2 that fail to form the intramolecular disulfide bridge are potent inducers of motor neuron differentiation, and gain independence from Prdx1 regulation. Our findings extend to the control of spinal interneuron differentiation, implicating thiol redox pathways as key controllers of neuronal differentiation in the spinal cord.

Results

The antioxidant enzyme Prdx1 interacts with GDE2

To identify molecules that regulate GDE2 function, we carried out unbiased screens for GDE2 interacting proteins using large-scale immunoprecipitation (IP) of FLAG-tagged GDE2

containing complexes followed by Liquid Chromatography-Mass Spectrometry/Mass Spectrometry (LC-MS/MS). Extracts derived from embryonic chick spinal cords electroporated with plasmids expressing FLAG-GDE2 were analyzed to identify neural specific GDE2 interactors, and extracts prepared from FLAG-GDE2 transfected HEK293T cells were utilized to identify general interactors of GDE2. LC-MS/MS analyses of component proteins from GDE2 complexes IPed from both sources identified Prdx1 as a GDE2 interacting protein (Figure 1A, B, E). We confirmed the interaction between Prdx1 and GDE2 by coIP, using extracts prepared from HEK293T cells transfected with epitope-tagged versions of Prdx1 and GDE2 (Figure 1G, Figure S2). GDE2 mutants lacking the intracellular N-terminal domain ($GDE2\Delta N^{38}$) failed to interact with Prdx1, indicating that Prdx1 associates with the N-terminal 38 amino acids of GDE2 (Figure 1G). Analyses of Prdx1 mRNA and protein on sections of chick embryonic spinal cord spanning the peak period of motor neuron differentiation show that Prdx1 is expressed in progenitor cells located in the VZ prior to the onset of GDE2 expression, but overlaps with GDE2 in IZ cells and postmitotic motor neurons in the MZ (Figure 1C, D, F).

Prdx1 is required for motor neuron differentiation

The coincident expression of Prdx1 and GDE2 and their ability to associate raise the possibility that Prdx1/GDE2 complexes function to control motor neuron differentiation. To determine the consequences of loss of Prdx1 on spinal motor neuron differentiation, we ablated *Prdx1* expression in vivo. 21bp double-stranded RNA oligonucleotides designed against the Prdx1 coding sequence were electroporated into developing chick spinal cords at Hamburger Hamilton stage (St) 11, prior to the initiation of motor neuron differentiation (Rao et al., 2004). Embryos electroporated with *Prdx1* siRNA showed complete ablation of *Prdx1* mRNA expression and a dramatic reduction in Prdx1 protein (Figure 2A, B).

Immunohistochemical analyses of motor neuron progenitor and postmitotic markers on serial sections of embryos electroporated with *Prdx1* siRNA show that Prdx1 silencing caused the loss of approximately 50% of $Islet1^+$, $HB9^+$ and $Islet2^+$ motor neurons but did not alter the number of $Olig2^+$ motor neuron progenitors or the dorsal-ventral patterning of spinal progenitors (Figure 2C–G; Figure S3). No increase in TUNEL staining was detected, suggesting that the loss of Prdx1 did not compromise motor neuron survival (Figure S4). This is in contrast with siRNA ablation of *Gde2*, and may reflect additional functions for GDE2 in postmitotic motor neurons (Rao and Sockanathan, 2005). The siRNA-dependent silencing of *Prdx1* is specific as *Prdx1* knockdown could be titrated using differing amounts of *Prdx1* siRNA; unrelated siRNAs did not trigger *Prdx1* silencing; *Prdx1* siRNA did not induce global changes in gene expression, and coelectroporation of constructs expressing human Prdx1, which is insensitive to the siRNA, rescued the motor neuron phenotype (Figures S3, S5). Thus, Prdx1 is required for the formation of postmitotic motor neurons but not for earlier events in motor neuron progenitor specification, similar to the function of GDE2 (Rao and Sockanathan, 2005).

Aged *Prdx1* null mice develop haemolytic anaemia and acquire multiple malignancies, indicative of a tumor suppressor function for Prdx1 (Neumann et al., 2003; Egler et al., 2005). To determine if $Prdx1^{-/-}$ animals exhibit deficits in spinal motor neuron development, we analyzed $Prdx1^{-/-}$ embryos at E9.5 during the peak period of motor neuron differentiation. $Prdx1^{-/-}$ animals do not express *Prdx1* transcripts consistent with previous studies demonstrating the absence of Prdx1 protein in these mutants (Figure 3A, E; Neumann et al., 2003; Egler et al., 2005). $Prdx1^{-/-}$ mutants revealed similar phenotypes to chick embryos electroporated with *Prdx1* siRNAs. $Prdx1^{-/-}$ embryos lost approximately 50% of Islet1/$Islet2^+$ and $HB9^+$ motor neurons compared to WT littermates, while dorsal-ventral patterning events and the numbers of $Olig2^+$ progenitors were normal (Figure 3B–D, F, G; Figure S3).

Towards the end of the cell death phase at E16.5, *Prdx1* nulls and WT embryos had equivalent numbers of motor neurons (data not shown). The incomplete ablation of motor neurons in *Prdx1*$^{-/-}$ embryos may be a consequence of redundant functions of other Prdx proteins that regulate cellular differentiation such as Prdx2, which is expressed in the ventral mouse spinal cord and is capable of binding GDE2 or alternatively, redundancy with other known signaling pathways that regulate differentiation in the spinal cord (Figure S6; Choi et al., 2005).

TUNEL analysis showed no difference in cell death between *Prdx1*$^{-/-}$ and WT embryos, suggesting that Prdx1 regulates the differentiation of motor neurons rather than their survival (Figure S4). To explore this possibility in more detail, we compared the frequency of cell-cycle exit between *Prdx1*$^{-/-}$ and WT embryos at the peak period of motor neuron differentiation. We injected pregnant dams with BrdU to label cells in S phase, harvested embryos 16 hours later, and calculated the cell-cycle exit index by analyzing the ratio of non-proliferating to proliferating BrdU^{+} cells in the ventral spinal cord. At E9.5, there was a marked reduction in the cell-cycle exit index of *Prdx1*$^{-/-}$ embryos compared with WT littermates, but no differences in independent studies of cell-cycle progression at S and M phase (Figure 3H-N). Thus, Prdx1 is required for the differentiation of postmitotic motor neurons during the peak period of neurogenesis, but not for motor neuron progenitor specification or proliferation.

Prdx1 synergizes with GDE2 to drive spinal neuron differentiation

The similarity between the loss of function phenotypes between Prdx1 and GDE2 suggests that they operate within the same pathway to regulate motor neuron differentiation. To test this possibility, we carried out gene dosage experiments by generating mice heterozygous for *Gde2* and *Prdx1*. At the peak of spinal motor neuron differentiation, WT, *Prdx1*$^{+/-}$ and *Gde2*$^{+/-}$ animals contain comparable numbers of Olig2^{+} motor neuron progenitors and HB9^{+} and Islet1/2^{+} motor neurons (Figure 3O-U). In contrast, double heterozygous *Prdx1*$^{+/-}$*; Gde2*$^{+/-}$ embryos exhibit an approximately 40% and 30% reduction in HB9^{+} and Islet1/2^{+} motor neurons respectively, while retaining equivalent numbers of Olig2^{+} motor neuron progenitors to controls (Figure 3P, T, R). This observation provides strong genetic evidence that Prdx1 and GDE2 function within the same pathway to control motor neuron differentiation.

To investigate the synergy between Prdx1 and GDE2 in promoting motor neuron differentiation, we performed in vivo gain of function assays using in ovo electroporation of embryonic chick spinal cords. We engineered expression constructs placing an HA-tagged version of Prdx1 under the control of the chick β-actin promoter (pCAGGS-Prdx1) and bicistronic constructs expressing GDE2 (pCAGGS-GDE2IRESLacZ). As described previously, overexpression of GDE2 in cycling progenitors caused many cells to differentiate into postmitotic motor neurons prematurely; in contrast, overexpression of Prdx1 induced very few Islet1/2^{+} motor neurons (Figure 4A, B O; Rao and Sockanathan, 2005). To determine if Prdx1 and GDE2 cooperate to induce motor neuron differentiation, we coexpressed Prdx1 and a suboptimal amount of GDE2 in the spinal cord that normally does not give rise to motor neurons (0.5 X GDE2; Figure 4C, O). Coelectroporation of Prdx1 and GDE2 generated many ectopic Islet1/2^{+} motor neurons in the VZ in numbers that exceeded that of Islet1/2^{+} cells induced when optimal amounts of GDE2 alone are electroporated (Figure 4A, D, O). The ectopic Islet1/2^{+} motor neurons bore the hallmarks of motor neurons generated by GDE2 activity: they had downregulated progenitor markers such as Sox1 and Olig2, they had exited the cell-cycle as assessed by the lack of BrdU incorporation, and they expressed the postmitotic marker p27 and the motor neuron markers, Islet2 and HB9 (Figure 4I–L; data not shown; Rao and Sockanathan, 2005). Furthermore, 30% of the ectopic motor neurons did not express Prdx1 or GDE2, consistent with the ability of GDE2 to promote non cell-autonomous motor neuron differentiation (Figure 4M, N; Rao and Sockanathan, 2005). Thus, Prdx1 synergizes with

GDE2 to promote motor neuron differentiation in vivo. Prdx2 can similarly cooperate with GDE2 to drive motor neuron differentiation, consistent with redundant functions for 2-Cys Prdx proteins in controlling GDE2-dependent motor neuron differentiation (Figure S6).

Strikingly, coexpression of Prdx1 and GDE2 in the dorsal spinal cord led to a similar induction of p27 and concomitant downregulation of Sox1 in VZ progenitors, (Figure 5A–D). Further, these medially located postmitotic cells expressed appropriate postmitotic interneuron markers specific to their dorsal-ventral position, suggesting that Prdx1 and GDE2 cooperate to promote the differentiation of diverse interneuron subtypes (Figure 5E–I). This observation is consistent with the dorsal expression of Prdx1 in IZ cells, and the dorsal expansion of GDE2 expression, which coincides with the temporal profile of spinal neurogenesis. In support of this model, ablation of *Prdx1* expression by siRNA caused a loss of dI2-d6 dorsal interneurons and ventral interneuron subclasses, suggesting general roles for GDE2 and Prdx1 in controlling neuronal differentiation in the spinal cord (Figure 5J–Q).

Prdx1/GDE2 properties necessary for motor neuron induction

We utilized the synergistic gain of function assay to define the basis of the cooperativity between GDE2 and Prdx1. To determine if physical interaction between GDE2 and Prdx1 is required for premature motor neuron induction, we coelectroporated expression constructs for Prdx1 and GDE2ΔN^{38} into chick spinal cords. GDE2ΔN^{38} lacks the Prdx1 interaction domain and is expressed and transported to the membrane at similar levels as GDE2 (Figures 1 and S7). Coexpression of GDE2ΔN^{38} and Prdx1 failed to induce ectopic Islet1/2^{+} motor neurons in the VZ, suggesting that Prdx1 functions in a complex with GDE2 to regulate motor neuron differentiation (Figure 4E, O). Both GDE2 and Prdx1 contain catalytic domains that are essential for their functions. Mutation of a histidine residue to alanine within the GDE2 GDPD domain severely impairs its ability to drive motor neuron differentiation (GDE2H^{275A}), while mutation of the reactive Cys (Prdx1C$^{52.173S}$) or an arginine residue located near the Prdx1 active site (Prdx1R^{128E}) abolishes Prdx1 catalytic activity (Jang et al., 2004; Zheng et al., 2003; Rao and Sockanathan, 2005; Montemartini et al., 1999; Flohe et al., 2002). CoIP assays show that GDE2H^{275A}, Prdx1C$^{52.173S}$ and Prdx1R^{128E} retain their ability to form complexes with WT Prdx1 and GDE2 respectively (Figure S8). GDE2H^{275A} did not synergize with Prdx1 to promote premature motor neuron differentiation, while coexpression of Prdx1C$^{52.173S}$ or Prdx1R^{128E} with GDE2 in chick spinal cords did not induce ectopic Islet1/2^{+} motor neurons in the VZ (Figure 4F–H, O). These observations confirm that GDE2 GDPD activity is required for GDE2/Prdx1 complexes to promote motor neuron differentiation. Moreover, they reveal that Prdx1 catalytic activity is required for the ability of GDE2 to regulate motor neuron differentiation, and further argue against a molecular chaperone function for Prdx1 in this context, as Prdx1C$^{52.173S}$ mutants retain effective chaperone activity in the absence of elevated H_2O_2 (Jang et al., 2004).

Prdx1 reduces an intramolecular disulfide bond within GDE2

How does Prdx1 catalytic activity regulate GDE2 function? The yeast Gpx3 and TSA peroxiredoxins can induce disulfide bond formation in the redox-response transcription factor Yap1 under conditions of oxidative stress, while the bacterial peroxiredoxin AhpC has in vitro disulfide reductase activity (Delaunay et al., 2002; Ritz et al., 2001). To evaluate if Prdx1 is capable of modifying GDE2 disulfide bond formation, we compared the presence of free thiol groups in GDE2 in the absence or presence of Prdx1 using 4-acetamido-4′-maleimidylstilbene-2,2′-disulfonic acid (AMS), a thiol-conjugating reagent that decreases the electrophoretic mobility of bound proteins by 0.5kDa/free thiol (Sevier et al., 2007). Western blot analyses of deglycosylated surface biotinylated GDE2 in HEK293T cells showed a decrease in GDE2 mobility in the presence of AMS, indicating that GDE2 at the cell surface normally contains free thiols (Figure 6A). When Prdx1 is coexpressed with GDE2, there was

a small but reproducible shift in the mobility of GDE2 by AMS modification consistent with an increase of free thiol groups (Figure 6A). The Prdx1-dependent decrease in GDE2 mobility requires Prdx1 redox activity since the catalytically inactive Prdx1C$^{52.173S}$ mutant fails to alter GDE2 migration (Figure 6A).

GDE2 contains 3 closely spaced Cys residues within its intracellular N-terminal region (C15, C18, C25) and 1 Cys within its C-terminal domain (C576) (Figure 6B). To identify the Cys residues reduced by Prdx1, we mutated the C15 and C18 residues (GDE2C$^{15.18S}$), and the C25 and C576 residues (GDE2C$^{25.576S}$) of GDE2 to serine. Both GDE2C$^{15.18S}$ and GDE2C$^{25.576S}$ retained the ability to bind Prdx1 and are expressed at the membrane at equivalent levels (Figures S7, S9). Coexpression of Prdx1 and GDE2C$^{15.18S}$ in HEK293T cells caused a shift in GDE2 mobility by AMS modification, similar to that observed when Prdx1 and WT GDE2 are cotransfected (Figure 6A). Since C25 and C576 are the only intracellular thiol groups available in GDE2C$^{15.18S}$, this result suggests that Prdx1 causes the reduction of a disulfide bond normally formed between the C25 and C576 residues of GDE2. Consistent with this observation, Prdx1 did not alter the mobility of GDE2C$^{25.576S}$ modified by AMS (Figure 6A).

To investigate the effect of Prdx1 on GDE2 further we utilized biochemical assays adapted to detect the presence of disulfide bonds in GDE2 in transfected HEK293T cells (Leichert and Jakob, 2004). Free thiol groups in GDE2 were blocked by N-ethylmaleimide (NEM) prior to the stepwise addition of Tris (2-carboxyethyl) phosphine (TCEP) and N-(6-(Biotinamido) hexyl)-3′-(2′-pyridyldithio)-propionamide (Biotin-HPDP), which respectively causes the reduction of disulfide bonds and the modification of resultant free thiols by biotin. Western blotting of IPed GDE2 shows that in the absence of TCEP, GDE2 was not labeled by biotin, demonstrating effective blockade of free thiols in GDE2 (Figure 6C). Addition of TCEP resulted in biotinylated GDE2, consistent with the reduction and labeling of endogenous disulfide bonds in GDE2 (Figure 6C, GFP). However, coexpression of Prdx1 with GDE2, but not the redox-inactive Prdx1C$^{52.173S}$ mutant, decreased the amount of biotinylated GDE2, suggesting that Prdx1 catalytic activity causes reduction of disulfide bonds within GDE2 (Figure 6C). Analysis of GDE2 Cys mutants showed that while a similar reduction of biotinylated GDE2C$^{15.18S}$ was observed in the presence of Prdx1, no changes in biotin labeling of GDE2C$^{25.576S}$ was detected (Figure 6C), consistent with our AMS data and the model that Prdx1 can cause reduction of the C25-C576 disulfide bond in GDE2.

The C25-C576 disulfide bridge is unusual given the reducing environment of the cell; thus, we utilized LC-MS/MS to confirm that C25 and C576 participate in disulfide bond formation in transfected HEK293T cells. Free thiol groups were blocked by NEM prior to reduction by DTT and subsequent thiol modification by iodoacetamide (IAM). LC-MS/MS analysis revealed that C576 was labeled by NEM and IAM, suggesting that C576 participates in disulfide bond formation and that this disulfide bond is dynamic (Figure 6E, Figure S10). To examine if Prdx1 leads to the reduction of GDE2 disulfide bonds utilizing C576, we compared the relative signal intensities of GDE2 peptides containing C576 NEM and C576 IAM by LC-MS/MS in the absence and presence of Prdx1. In the absence of Prdx1, the relative intensities of both peptides were approximately similar. GDE2 and Prdx1 coexpression led to a 5–6 fold increase of C576 NEM labeling compared with C576 IAM, suggesting that Prdx1 shifts the equilibrium of C576 to a reduced state (Figure 6E). In addition, LC-MS/MS analysis showed that C25 can be labeled by IAM (data not shown). These collective observations are consistent with our AMS and biotin labeling experiments, and support the model that Prdx1 catalytic activity causes reduction of an intramolecular disulfide bond formed between C25 and C576 of GDE2.

Prdx1 and GDE2 form a disulfide intermediate

If Prdx1 directly reduces a disulfide bond formed between C25 and C576 in GDE2, then GDE2 and Prdx1 should form a transient mixed-disulfide intermediate during the transfer reaction (Sevier et al., 2002). To address this question, we coIPed GDE2 containing complexes from extracts prepared from HEK293T cells transfected with Prdx1 and GDE2. Analysis of Prdx1 redox state in transfected extracts shows that Prdx1 exists in reduced and oxidized forms (Figure S8). Western blots show that forms of Prdx1 associated with GDE2 include reduced monomers, high molecular weight complexes and a band of approximately 120–130kDa that corresponds to the predicted molecular weight of a GDE2/Prdx1 complex (open circles, arrow, Figure 6D). Addition of β-mercaptoethanol abolished formation of the 120–130kDa complex, suggesting that its assembly utilizes disulfide bonds (Figure 6D). Coexpression of GDE2 and Prdx1C$^{52.173S}$, or GDE2C$^{25.576S}$ and Prdx1, failed to form the 120–130kDa complex although Prdx1C$^{52.173S}$ and GDE2C$^{25.576S}$ retain their abilities to bind GDE2 and Prdx1 respectively (Figures 6D, S8, S9). In contrast, GDE2C$^{15.18S}$, which preserves the capacity to form an intracellular disulfide bond between C25 and C576, can form the 120–130kDa complex (Figure 6D). These observations suggest that the 120–130kDa complex is a mixed-disulfide Prdx1-GDE2 intermediate, and that the cysteines responsible for Prdx1 redox activity, and the C25 or C576 residue in GDE2, participate in its formation.

GDE2C$^{25.576S}$ is a potent inducer of differentiation that is independent of Prdx1

Our developmental and biochemical studies are consistent with the model that Prdx1 directly activates GDE2 by reducing an intracellular C25-C576 disulfide bond that bridges the N and C-terminal domains of GDE2. If so, then GDE2C$^{25.576S}$, which cannot form the disulfide bridge, should be more effective than GDE2 in promoting motor neuron differentiation. In addition, GDE2C$^{25.576S}$ should no longer cooperate with Prdx1 to induce ectopic motor neurons in the VZ. To evaluate the activity of GDE2C$^{25.576S}$, we compared the ability of GDE2C$^{25.576S}$ and GDE2 to induce ectopic Islet2^{+} motor neurons in the VZ of embryonic chick spinal cords, using suboptimal amounts of GDE2 that normally fail to elicit premature motor neuron differentiation (Figure 4C, O; Figure 7A, C, G, H). In contrast to GDE2, electroporation of suboptimal amounts of pCAGGS-GDE2C$^{25.576S}$ effectively induced the differentiation of Islet2^{+} motor neurons in VZ progenitors (Figure 7C). Variants of GDE2 that contained a single point mutation converting the C25 or C576 residue to serine (GDE2C^{25S}, GDE2C^{576S}) were similarly effective (Figure 7D, E, G, H). However, expression of GDE2C$^{15.18S}$, which retains the ability to form the C25-C576 disulfide bridge, showed similar activity as GDE2 in promoting motor neuron differentiation under these conditions (Figure 7B, G, H). Surface biotinylation and expression studies in transfected HEK293T cells showed that GDE2, GDE2C$^{25.576S}$, GDE2C^{25S}, GDE2C^{576S} and GDE2C$^{15.18S}$ are expressed at similar levels on the cell membrane (Figure S7). These findings extend to the differentiation of dorsal and ventral spinal interneurons, and thus collectively imply that reduction of the C25-C576 disulfide bond between the N and C-terminal domains of GDE2 increases the efficacy of GDE2 to promote neuronal differentiation, suggesting that the C25-C576 bridge normally gates GDE2 function (Figure 7I-P).

To test if GDE2 mutants that fail to form the C25-C576 bridge cooperate with Prdx1 to promote motor neuron differentiation, we electroporated suboptimal amounts of pCAGGS-GDE2C^{25S} into embryonic chick spinal cords, and compared the ability of GDE2C^{25S} to induce ectopic motor neurons in the absence or presence of Prdx1. GDE2C^{25S} is capable of binding Prdx1 and effectively induced Islet2^{+} motor neurons in the VZ (Figure 7E, G, H; Figure S9). However, Prdx1 failed to potentiate the ability of GDE2C^{25S} to induce ectopic motor neurons, suggesting that GDE2C^{25S} does not require Prdx1 activity to drive motor neuron differentiation (Figure 7F, G, H). This finding suggests that the major function of Prdx1 in the context of the

Prdx1/GDE2 complex is to reduce the C25-C576 disulfide bridge that normally gates the ability of GDE2 to drive motor neuron differentiation.

Discussion

The antioxidant scavenger Prdx1 plays critical roles in the defense of oxidative and thermal stress by its diverse abilities to respectively metabolize H_2O_2 and act as a molecular chaperone (Wood et al., 2003; Rhee et al., 2005; Jang et al., 2004). Using spinal motor neuron differentiation as a model system, we have uncovered a previously uncharacterized developmental role for Prdx1 in controlling neuronal differentiation. Our study suggests a model where the overlap of Prdx1 and GDE2 expression in cells neighboring VZ progenitors permits the association of Prdx1 with GDE2 (Figure 7Q). GDE2 is normally inactive due to the presence of an intramolecular disulfide bond that links its intracellular N and C-terminal domains. However, once complexed with GDE2, Prdx1 catalytic activity leads to reduction of the GDE2 C25-C576 disulfide bond and activation of GDE2, triggering motor neuron differentiation through extracellular GDE2 GDPD metabolism (Figure 7Q). These findings uncover critical roles for thiol-redox dependent mechanisms in activating GDE2 signaling, and identify peroxiredoxins as pivotal regulators of neuronal differentiation in the spinal cord.

Several lines of evidence suggest the intriguing possibility that the requirement for Prdx1 in motor neuron differentiation stems from a previously uncharacterized enzymatic function that is distinct from its molecular chaperone or H_2O_2 metabolic activities. First, Prdx1 mutants that retain effective molecular chaperone activity but are catalytically inactive do not synergize with GDE2 to drive premature motor neuron differentiation in VZ progenitors. Second, loss of Prdx1 causes a deficit of postmitotic motor neurons in the absence of cell death. This observation is consistent with a role for Prdx1 in regulating motor neuron differentiation, and argues against the possibility that motor neuron survival is compromised through increased ROS levels stemming from loss of Prdx1 scavenger function. Third, our data suggests that Prdx1 activates GDE2 through thiol reductase mechanisms that might not utilize H_2O_2 as a substrate, as thiol modifications that utilize H_2O_2 metabolism are consistent with oxidation rather than reduction. Although our data do not rule out the formal possibility that Cys25 and Cys576 form sulfenic acids rather than a disulfide bond, this appears unlikely as sulfenic acids are considered very unstable and do not form when in close proximity to other Cys residues (Paget and Buttner, 2003). Our study thus poses a potential role for Prdx1 in directly regulating the activity of target proteins through disulfide bond reduction. In support of the dual enzymatic capabilities of peroxiredoxins, bacterial AhpC, a typical 2-Cys peroxiredoxin like Prdx1, exhibits disulfide reductase activity in vitro, and can function as a biologically active disulfide reductase by the addition of a single amino acid (Ritz et al., 2001). Nevertheless, confirmation of the possible disulfide reductase activity of Prdx1 awaits further investigation.

Actively cycling progenitors are inherently responsive to GDE2 GDPD differentiation signals and can undergo terminal differentiation if prematurely exposed to GDE2 activity (Rao and Sockanathan, 2005). Thus, the precise regulation of GDE2 activity is crucial to limit the exposure of GDPD differentiation signals to only those progenitors that are poised to undergo differentiation (Rao and Sockanathan, 2005). Our study suggests that this is accomplished in part by the coexpression of Prdx1 and GDE2 in IZ cells throughout the spinal cord, which restricts the formation of active Prdx1/GDE2 complexes and the subsequent production of GDPD differentiation signals to progenitors at the lateral margin of the VZ. Other strategies to ensure a restricted zone of GDPD-dependent signaling likely include mechanisms to downregulate GDE2 activity. This could occur through the targeted degradation of active, reduced disulfide forms of GDE2 through endocytic pathways; however, our surface biotinylation studies argue against this scenario as WT and hyperactive forms of GDE2 are present at equivalent amounts on the cell membrane. An alternative mechanism to

downregulate GDE2 activity is to regenerate the GDE2 C25-C576 disulfide bridge through thiol oxidation. This mechanism poses that the C25-C576 disulfide bridge functions as a reversible thiol-dependent switch to control GDE2 function, and invokes the existence of thiol oxidative proteins that negatively regulate GDE2 function.

Such redox-dependent recycling mechanisms are also likely to apply to Prdx1. Prdx1-dependent activation of GDE2 should result in the oxidation of the Prdx1 reactive Cys and inactivation of Prdx1 catalytic activity. Consistent with this model, coexpression of Prdx1 and GDE2 increases the amount of oxidized Prdx1 (Figure S8). This implies that the progression of neuronal differentiation relies upon the effective recycling of Prdx1 to active reduced forms. Obvious candidates for reactivating Prdx1 include members of the Trx family of proteins, which are known electron donors for Prdx1 (Rhee et al., 2005; Arnér and Holmgren, 2006). The need to recycle Prdx1 and downregulate GDE2 activity thus predicts that a cascade of coupled thiol redox-dependent pathways plays central roles in regulating the onset and progression of motor neuron differentiation in the spinal cord.

Our studies suggest that GDE2/Prdx1 complexes are not limited to controlling motor neuron differentiation but that they also regulate the differentiation of dorsal and ventral spinal interneurons. Our findings thus have potential implications for understanding general mechanisms that govern the transition between cellular proliferation and differentiation. In the developing spinal cord, progenitor proliferation is controlled by canonical Wnt signaling pathways (Megason and McMahon, 2002; Zechner et al., 2003). A recent report reveals that Nucleoredoxin, a Trx family member, inhibits proliferation by negatively regulating β-catenin mediated Wnt signaling through interactions with Dishevelled (Funato et al., 2006). This observation taken together with our study, suggests the compelling possibility that Trx-Prdx coupled pathways form a thiol redox-dependent cascade that triggers the onset of neuronal differentiation in the spinal cord. Trx proteins may have dual roles in inhibiting Wnt-dependent progenitor proliferation and ensuring the availability of reduced forms of Prdx proteins, which in turn, activate key modulators of differentiation such as GDE2. Trx and Prdxs are widely expressed, while GDE2 and its family members are expressed in other regions of the central nervous system and non-neural tissues such as the heart, lung, gut and bone (Rhee et al., 2005; Yanaka et al., 2003; Rao and Sockanathan, 2005). The conservation of the N- and C-terminal Cys residues in GDE3 and GDE6, together with the coincident distribution of Trx, 2-Cys Prdxs and six-transmembrane GDPD proteins in varied cell types suggests that coupled thiol-redox regulation of GDPD signaling may constitute a key mechanism for regulating cellular differentiation in diverse cellular contexts.

Experimental procedures

Immunoprecipitation and LC-MS/MS

N-terminal FLAG-tagged GDE2 or control vector was transfected into HEK293T cells or electroporated into approximately 150–200 St 13 embryonic chick spinal cords. Cell extracts and spinal cord lysates were harvested 24hrs later and subjected to IP by anti-FLAG M2 Affinity gel (Sigma). Protein complexes were resolved by SDS-PAGE, silver stained and GDE2 specific bands were excised and subjected to LC-MS/MS (Taplin Biological Mass Spectrometry Facility, Harvard Medical School).

In situ hybridization and immunofluorescence

In situ hybridization and immunostaining analyses were performed as previously described (Rao and Sockanathan, 2005). Details of antibodies are provided in supplemental material. TUNEL analysis was performed using the ApopTag fluorescein in situ apoptosis detection kit

(Chemicon S7110). Confocal micrographs were captured on a Zeiss LSM 5 PASCAL microscope.

Loss and gain-of-function experiments

Chick embryos were electroporated with siRNA (Rao et al., 2004) and analyzed 40 hours later at St19-21. 10–20 sections from each of 6 embryos with at least 80% loss of *Prdx1* mRNA expression were scored. *GDE2*$^{+/-}$ animals were generated by standard procedures involving targeted recombination of the *GDE2* locus in ES cells. Disruption of the *GDE2* allele in animals was confirmed by Southern blotting, PCR, and immunohistochemistry. For *GDE2*$^{+/-}$ and *Prdx1* null mutant analyses, 15–20 sections from 5 embryos were counted.

For gain-of-function experiments, electroporated embryos were BrdU labeled to define the lateral extent of the VZ (Rao and Sockanathan, 2005). Images of 10–20 sections/embryo (n=5–10 embryos) were scored. Sections were chosen to ensure equivalent electroporation efficiency by LacZ (GDE2) and HA (Prdx1) staining. All mutant and deletion constructs were generated by site-directed (Quickchange kit, Stratagene) or PCR based mutagenesis.

Cell-cycle analysis

Pregnant dams were injected with BrdU (100mg/kg body weight) 30 min and 16 hours prior to embryo harvest for calculation of S-phase and cell-cycle exit indices respectively. S-phase: BrdU^{+}/Ki67^{+} cells where Ki67 marks all cycling cells; cell-cycle exit: BrdU^{+}, Ki67^{-}/BrdU^{+}, Ki67^{+}; mitotic index: Mpm2^{+}/Ki67^{+}, where Mpm2 marks cells in mitosis (Chenn and Walsh, 2002).

Biochemical experiments

CoIP studies using FLAG-GDE2 and HA- or myc-Prdx1 transfected in HEK-293 cells were performed with GammaBind G sepharose beads (Amersham). Western blotting was performed using HA-HRP (F7, 1:10,000, Santa Cruz) or polyclonal GDE2 antibodies (1:200,000).

GDE2 oxidation states were analyzed by redox western blots on surface biotinylated GDE2 protein in transfected HEK293T cells. Transfected cells were washed with cold PBS and biotinylated with sulfo-NHS-SS-Biotin (Pierce) (1mg/ml) at 4°C for 30 min. Cells were treated with 10% (w/v) trichloroacetic acid (4°C, 30 min), and proteins were centrifuged and washed with 100% acetone. Protein precipitates were suspended in 80mM Tris-HCl pH6.8, 2% SDS, 6M urea, 1mM PMSF with 20mM AMS (Molecular probes) and the samples adjusted to neutral pH with 1M Tris-HCl pH7.5. AMS labeling was done on ice (15 min), 37°C (20 min), boiled for 2 min and samples IPed by immobilized monomeric avidin (Pierce). Eluted proteins were deglycosylated with 25U/μl PNGase F (New England Biolabs) before resolving by non-reducing SDS-PAGE. GDE2 was detected by western blotting using GDE2 antibodies.

To detect disulfide bonds, transfected cells were washed with cold PBS supplemented with 10mM NEM (Sigma), lysed in 10mM Tris pH7.0, 150mM NaCl, 1% NP-40, 0.1% SDS with 40mM NEM and proteinase inhibitors at 4°C for 30 min, and centrifuged. Supernatants were acetone precipitated at −20°C, washed with 70% acetone, resolubilized in HENS buffer (250mM Hepes pH7.7, 1mMEDTA, 1%SDS) with 5 mM TCEP, and incubated for 1 hr to reduce disulfide bonds. The reaction was quenched with acetone, and proteins were precipitated and washed as above. Pellets were resolubilized in HENS with 0.5 mM biotin-HPDP (Pierce). Biotin labeling was carried out at room temperature for 90min, the reaction quenched by acetone precipitation, and the pellet resolubilized in 25mM Hepes pH7.7, 0.1mMEDTA, 0.75% SDS and diluted with 6 volumes of 1%Triton in TBS. GDE2 was IPed using anti-Flag M2 Affinity gel and Western blots were probed with antibodies against Biotin (1:10,000, Sigma) and GDE2. GDE2 protein was similarly labeled for LC-MS/MS; however, 10mM DTT was

used instead of TCEP and 40mM IAM was used instead of Biotin-HPDP. GDE2 was IPed by anti-Flag M2 Affinity gel, resolved by SDS-PAGE and stained with coomassie blue. Cysteines were identified by LC-MS/MS (Taplin Biological Mass Spectrometry Facility).

Trapping of mixed disulfides between GDE2 and Prdx1 was performed by standard IP with anti-Flag M2 Affinity gel except that 100mM of the thiol-alkylating agent maleimide was present in all solutions to block free thiol groups and prevent thiol-disulfide exchange or thiol oxidation (Burgoyne et al., 2007). Protein complexes were eluted by non-reducing sample buffer and divided into two equal fractions, one of which was reduced with 10% β-ME before analysis by SDS-PAGE. Prdx1 and Prdx1-GDE2 disulfide intermediates were detected by western blotting using rabbit anti-HA antibodies (1:200, Y11, Santa Cruz).

Supplementary Material

Refer to Web version on PubMed Central for supplementary material.

Acknowledgments

We thank S. Lawson for technical assistance; J. Rotty for help in initial candidate screens; M. Goulding, T.M. Jessell, L. Pevny and B. Novitch for antibodies; E. Prochownik and Y.F. Shi for *Prdx1* null animals; C.H. Lee, G. Periz and B.Q. Zhuang for discussions; A.L. Kolodkin, G. Periz, W. Watson and P.F. Worley for critical reading and comments on the manuscript. This work was funded by the NINDS and the Muscular Dystrophy Association.

References

Arnér ES, Holmgren A. The thioredoxin system in cancer. Semin Cancer Biol 2006;16:420–426. [PubMed: 17092741]

Bertram JS. The molecular biology of cancer. Mol Aspects Med 2000;21:167–223. [PubMed: 11173079]

Burgoyne JR, Madhani M, Cuello F, Charles RL, Brennan JP, Schröder E, Browning DD, Eaton P. Cysteine Redox Sensor in PKGIa Enables Oxidant-Induced Activation. Science 2007;317:1393–1397. [PubMed: 17717153]

Chenn A, Walsh CA. Regulation of cerebral cortical size by control of cell cycle exit in neural precursors. Science 2002;297:365–369. [PubMed: 12130776]

Choi MH, Lee IK, Kim GW, Kim BU, Han YH, Yu DY, Park HS, Kim KY, Lee JS, Choi C, et al. Regulation of PDGF signalling and vascular remodelling by peroxiredoxin II. Nature 2005;435:347–353. [PubMed: 15902258]

Delaunay A, Pflieger D, Barrault MB, Vinh J, Toledano MB. A thiol peroxidase is an H_20_2 receptor and redox-transducer in gene activation. Cell 2002;111:471–481. [PubMed: 12437921]

Egler RA, Fernandes E, Rothermund K, Sereika S, de Souza-Pinto N, Jaruga P, Dizdaroglu M, Prochownik EV. Regulation of reactive oxygen species, DNA damage, and c-Myc function by peroxiredoxin 1. Oncogene 2005;24:8038–8050. [PubMed: 16170382]

Flohe L, Budde H, Bruns K, Castro H, Clos J, Hofmann B, Kansal-Kalavar S, Krumme D, Menge U, Plank-Schumacher K, et al. Tryparedoxin peroxidase of Leishmania donovani: Molecular cloning, heterologous expression, specificity and catalytic mechanism. Arch Biochem and Biophys 2002;397:324–335. [PubMed: 11795890]

Funato Y, Michiue T, Asashima M, Miki H. The thioredoxin-related redox-regulating protein nucleoredoxin inhibits Wnt-β-catenin signaling through Dishevelled. Nature Cell Bio 2006;8:501–508. [PubMed: 16604061]

Helms AW, Johnson JE. Specification of dorsal spinal cord interneurons. Curr Opin Neurobiol 2003;13:42–49. [PubMed: 12593981]

Hollyday M. Neurogenesis in the vertebrate neural tube. Int J Dev Neurosci 2001;19:161–173. [PubMed: 11255030]

Jang HH, Lee KO, Chi YH, Jung BG, Park SK, Park JH, Lee JR, Lee SS, Moon JC, Jeong WY, et al. Two enzymes in one: two yeast peroxiredoxins display oxidative stress-dependent switching from a peroxidase to a molecular chaperone function. Cell 2004;117:625–635. [PubMed: 15163410]

Jessell TM. Neuronal specification in the spinal cord: inductive signals and transcriptional codes. Nat Rev Genet 2000;1:20–29. [PubMed: 11262869]

Kintner C. Neurogenesis in embryos and in adult neural stem cells. J Neurosci 2002;22:639–643. [PubMed: 11826093]

Lee SK, Lee B, Ruiz EC, Pfaff SL. Olig2 and Ngn2 function in opposition to modulate gene expression in motor neuron progenitor cells. Genes and Dev 2005;19:282–294. [PubMed: 15655114]

Leichert LI, Jakob U. Protein thiol modifications visualized in vivo. PLoS Biology 2004:1723–1737.

Megason SG, McMahon AP. A mitogen gradient of dorsal midline Wnts organizes growth in the CNS. Development 2002;129:2087–2098. [PubMed: 11959819]

Mizuguchi R, Sugimori M, Takebayashi H, Kosako H, Nagao M, Yoshida S, Nabeshima Y, Shimamura K, Nakafuku M. Combinatorial roles of olig2 and neurogenin2 in the coordinated induction of pan-neuronal and subtype-specific properties of motoneurons. Neuron 2001;31:757–771. [PubMed: 11567615]

Montemartini M, Kalisz HM, Hecht HJ, Steinert P, Flohe L. Activation of site cysteine residues in the peroxiredoxin-type tryparedoxin peroxidase of Crithidia fasciculate Eur. J Biochem 1999;264:516–524.

Neumann CA, Krause DS, Carman CV, Das S, Dubey DP, Abraham JL, Bronson RT, Fujiwara Y, Orkin SH, Van Etten RA. Essential role for the peroxiredoxin Prdx1 in erythrocyte antioxidant defence and tumor suppression. Nature 2003;242:561–565. [PubMed: 12891360]

Nogusa Y, Fujioka Y, Komatsu R, Kato N, Yanaka N. Isolation and characterization of two serpentine membrane proteins containing glycerophosphodiester phosphodiesterase, GDE2 and GDE6. Gene 2004;337:173–179. [PubMed: 15276213]

Novitch BG, Chen AI, Jessell TM. Coordinate regulation of motor neuron subtype identity and pan-neuronal properties by the bHLH repressor Olig2. Neuron 2001;31:773–789. [PubMed: 11567616]

Novitch BG, Wichterle H, Jessell TM, Sockanathan S. A requirement for retinoic acid-mediated transcriptional activation in ventral neural patterning and motor neuron specification. Neuron 2003;40:81–95. [PubMed: 14527435]

Paget MS, Buttner MJ. Thiol-based regulatory switches. Annu Rev Genet 2003;37:91–121. [PubMed: 14616057]

Rao M, Baraban J, Rajaii F, Sockanathan S. In vivo comparative study of RNAi methodologies by in ovo electroporation in the chick embryo. Dev Dyn 2004;231:592–600. [PubMed: 15376322]

Rao M, Sockanathan S. Transmembrane protein GDE2 induces motor neuron differentiation in vivo. Science 2005;309:2212–2215. [PubMed: 16195461]

Rhee SG, Chae HZ, Kim K. Peroxiredoxins: A historical overview and speculative preview of novel mechanisms and emerging concepts in cell signaling. Free Rad Bio and Medicine 2005;38:1543–1552.

Ritz D, Lim J, Reynolds CM, Poole LB, Beckwith J. Conversion of a peroxiredoxin into a disulfide reductase by a triplet repeat expansion. Science 2001;294:158–160. [PubMed: 11588261]

Santelli E, Schwarzenbacher R, McMullan D, Biorac T, Brinen LS, Canaves JM, Cambell J, Dai X, Deacon AM, Elsliger MA, et al. Crystal structure of a glycerophosphodiester phosphodiesterase (GDPD) from Thermotoga maritima (TM1621) at 1.60 A resolution. Proteins 2004;56:167–170. [PubMed: 15162496]

Sevier CS, Qu H, Heldman N, Gross E, Fass D, Kaiser CA. Modulation of cellular disulfide-bond formation and the ER redox environment by feedback regulation of Ero1. Cell 2007;129:333–344. [PubMed: 17448992]

Sevier CS, Kaiser CA. Formation and transfer of disulphide bonds in living cells. Nat rev Mol Cell Bio 2002;3:836–847. [PubMed: 12415301]

Wood ZA, Schroder E, Harris JR, Poole LB. Structure, mechanism and regulation of peroxiredoxins. Trends in Biochem Sci 2003;28:32–40. [PubMed: 12517450]

Yanaka N, Imai Y, Kawai E, Akatsuka H, Wakimoto K, Nogusa Y, Kato N, Chiba H, Kotani E, Omori K, et al. Novel membrane protein containing glycerophosphodiester phosphodiesterase motif is transiently expressed during osteoblast differentiation. J Biol Chem 2003;44:43595–43602. [PubMed: 12933806]

Yanaka N, Nogusa Y, Fujioka Y, Yamashita Y, Kato N. Involvement of membrane protein GDE2 in retinoic acid-induced neurite formation in Neuro2A cells. FEBS Lett 2007;581:712–718. [PubMed: 17275818]

Yanaka N. Mammalian glycerophosphodiester phosphodiesterases. Biosci Biotechnol Biochem 2007;71:1811–1818. [PubMed: 17690467]

Zechner D, Fujita Y, Hülsken J, Müller T, Walther I, Taketo MM, Crenshaw EB 3rd, Birchmeier W, Birchmeier C. beta-Catenin signals regulate cell growth and the balance between progenitor cell expansion and differentiation in the nervous system. Dev Biol 2003;258:406–418. [PubMed: 12798297]

Zheng B, Berrie CP, Corda D, Farquhar MG. GDE1/MIR16 is a glycerophosphoinositol phosphodiesterase regulated by stimulation of G-protein coupled receptors. Proc Nat Acad Sci (USA) 2003;100:1745–1750. [PubMed: 12576545]

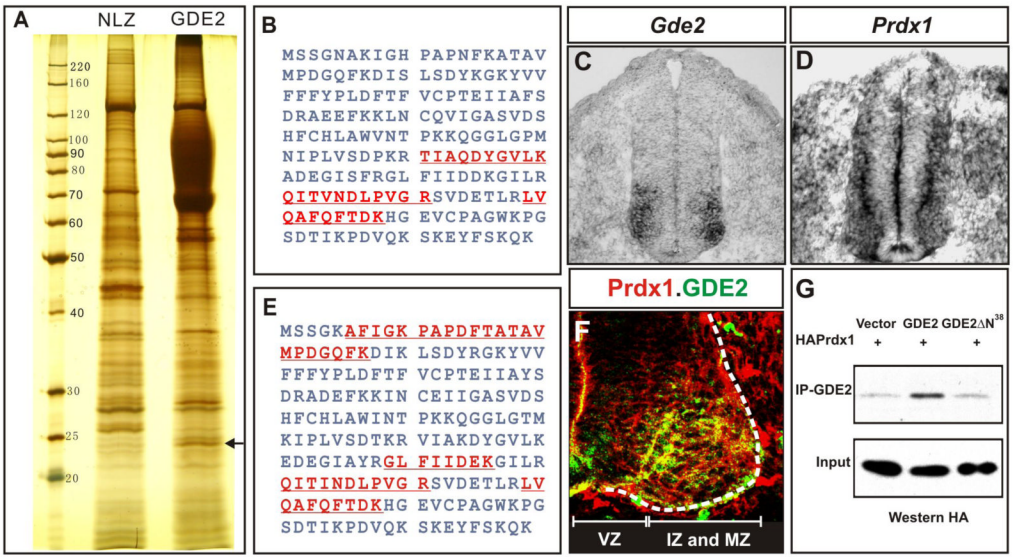

Figure 1. Prdx1 interacts and overlaps with GDE2 in the ventral spinal cord

(A) Silver stained SDS-PAGE gel shows a 23KDa band (arrow) coIPs with GDE2. NLZ, control plasmid; GDE2, pCAGGS-GDE2NLZ. (B, E) Tryptic peptides (red) from LC-MS/MS analyses of proteins derived from the 23KDa band correspond to human (B) and chick Prdx1 (E). (C, D, F) In situ hybridization of *Gde2* and *Prdx1* mRNA, and immunohistochemical analyses on transverse sections of St 19–20 chick spinal cords. Prdx1 and GDE2 proteins colocalize in intermediate (IZ) and marginal zone (MZ) cells but not in ventricular zone progenitors (VZ). (G) CoIPs of transfected HEK293T cells show HA-tagged Prdx1 interacts with the N-terminus of GDE2.

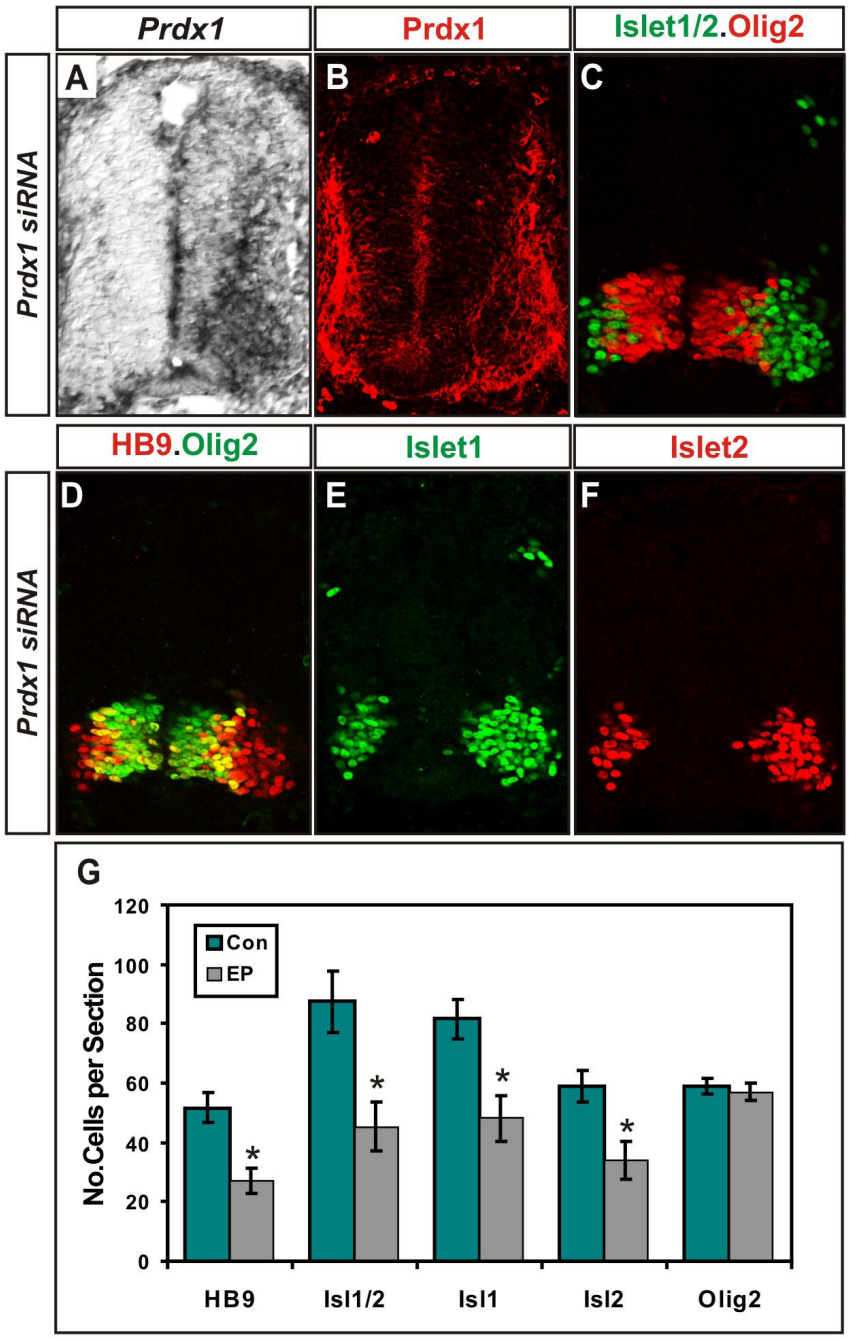

Figure 2. Prdx1 is required for motor neuron generation

(A) In situ hybridization and immunohistochemical analyses (B–F) of transverse sections of St 20–21 chick spinal cords electroporated with *Prdx1* siRNAs (left). $HB9^{+}$ motor neurons are visualized in red in D. (G) Graph shows reduction of postmitotic motor neurons on *Prdx1* silencing. Con= nonelectroporated side, EP= electroporated side (mean ± s.e.m.) * = HB9, p=0.000004; Islet1/2, p= 0.00001; Isl1, p=0.00009; Isl2, p= 0.00008; Olig2, p= 0.2; paired student's t-test, n= 6.

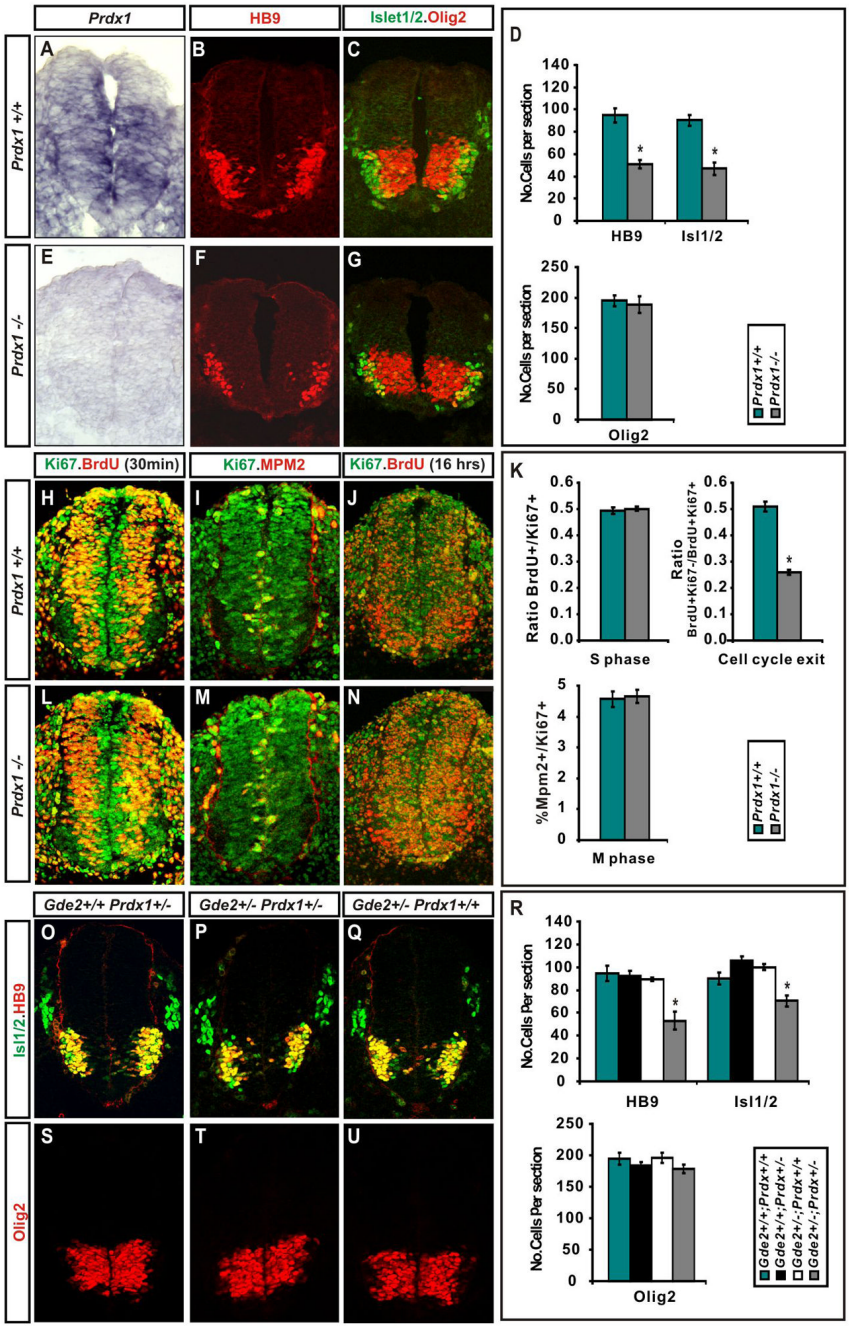

Figure 3. *Prdx1*$^{-/-}$ embryos show deficits in motor neuron generation

(A, E) In situ hybridization and (B, C, F, G, H–J, L–N) immunohistochemical analyses of transverse sections of mouse E9.5 *Prdx1*$^{+/+}$ and *Prdx1* null spinal cords. (D) Graphs show motor neuron loss in *Prdx1* nulls (mean ± s.e.m.) * HB9 p= 0.00054, * Isl1/2 p= 0.0004; Olig2 p= 0.69; two-tailed student's t-test, n= 5. (K) Graphs show deficits in cell-cycle exit in *Prdx1* nulls (mean ± s.e.m.) * = cell cycle exit, p= 0.0002, S-phase p= 0.63, M phase p= 0.8; two-tailed student's t-test, n= 5. (O-Q, S-U) Immunohistochemical analyses of transverse sections of mouse E9.5 spinal cords. (R) Graphs show motor neuron loss in double heterozygotes for *Prdx1* and *Gde2* (mean ± s.e.m.) 2 way ANOVA shows significant

interaction between GDE2 and Prdx1; *HB9 p= 0.00783, * Isl1/2 p= 6.54×10^{-5}, Olig2 p= 0.72; n= 5.

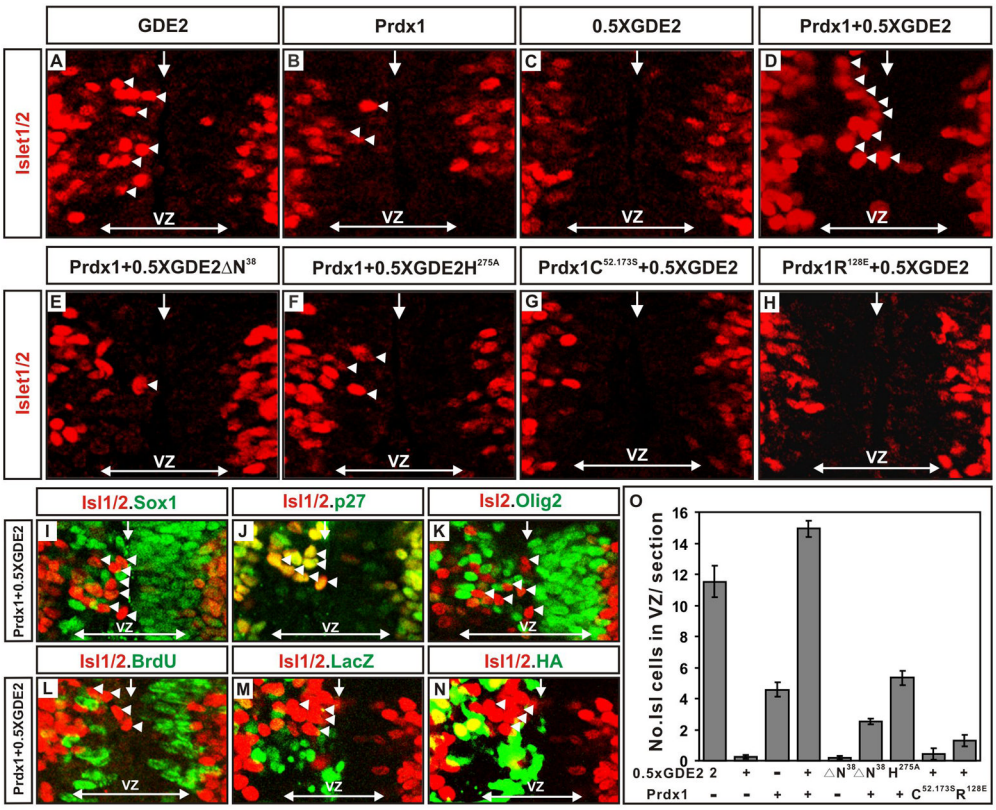

Figure 4. Prdx1/GDE2 complexes drive motor neuron differentiation in vivo

(A–N) Immunohistochemical analyses of transverse sections of ventral St 19–20 chick spinal cords electroporated (left) with GDE2 and Prdx1. Arrowheads mark terminally differentiated neurons in the ventricular zone (VZ). The VZ was defined by BrdU pulse labeling to mark S-phase cells at lateral margins. Midline: vertical arrow, VZ: horizontal arrow. (M, N) Same section stained with HA and LacZ to detect Prdx1 and GDE2 respectively (O) Graph quantifying ectopic motor neurons in the VZ of electroporated embryos (mean ± s.e.m; n= 5–10). Prdx1 overexpression weakly induces ectopic motor neurons, presumably through interactions with GDE2 related proteins in VZ cells such as GDE6 (C.H. Lee and S. Sockanathan; unpublished observations).

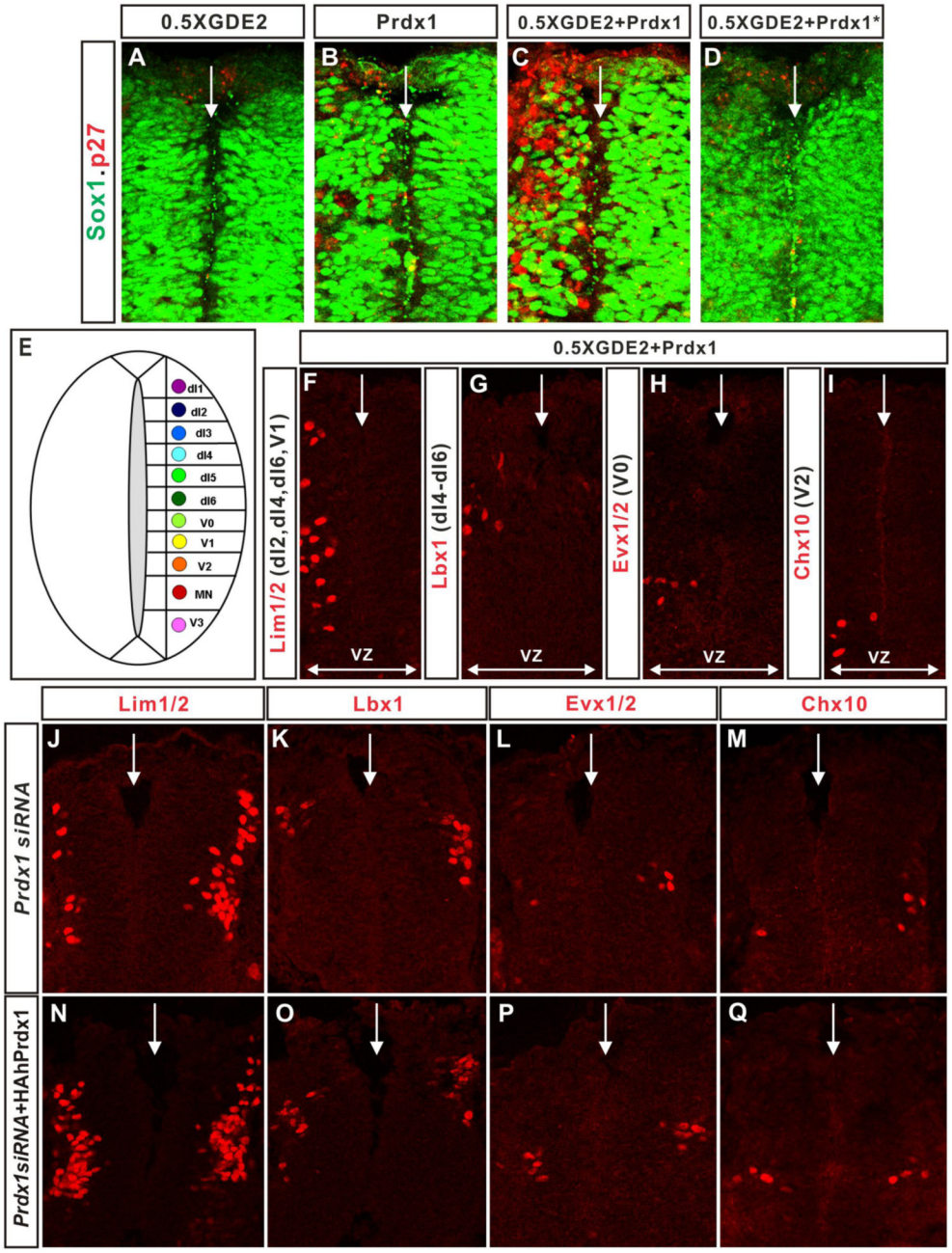

Figure 5. GDE2 and Prdx1 regulate spinal interneuron differentiation

(A–D; F–Q) Immunohistochemical analysis of transverse sections of St 20–21 dorsal chick spinal cords, electroporated on the left. Arrows mark the midline. VZ: ventricular zone, VZ extent = double headed arrows. Prdx1*=Prdx1C$^{52.173.S}$. (E) Schematic of the spinal cord showing the location of dorsal (dI1-6) and ventral (V0-V3) interneurons in relation to motor neurons (MN). (F-I) Prdx1 and GDE2 overexpression induces multiple interneuron subtypes in spinal progenitors [defined by their molecular gene expression profiles; Helms and Johnson, (2003)] within their respective dorsal-ventral domains. (J-M) Ablation of *Prdx1* by electroporation of siRNA reduces the number of dorsal and ventral spinal interneurons. (N-Q)

Spinal interneuron populations are rescued by electroporation of hPrdx1, which is insensitive to the electroporated *Prdx1* siRNA.

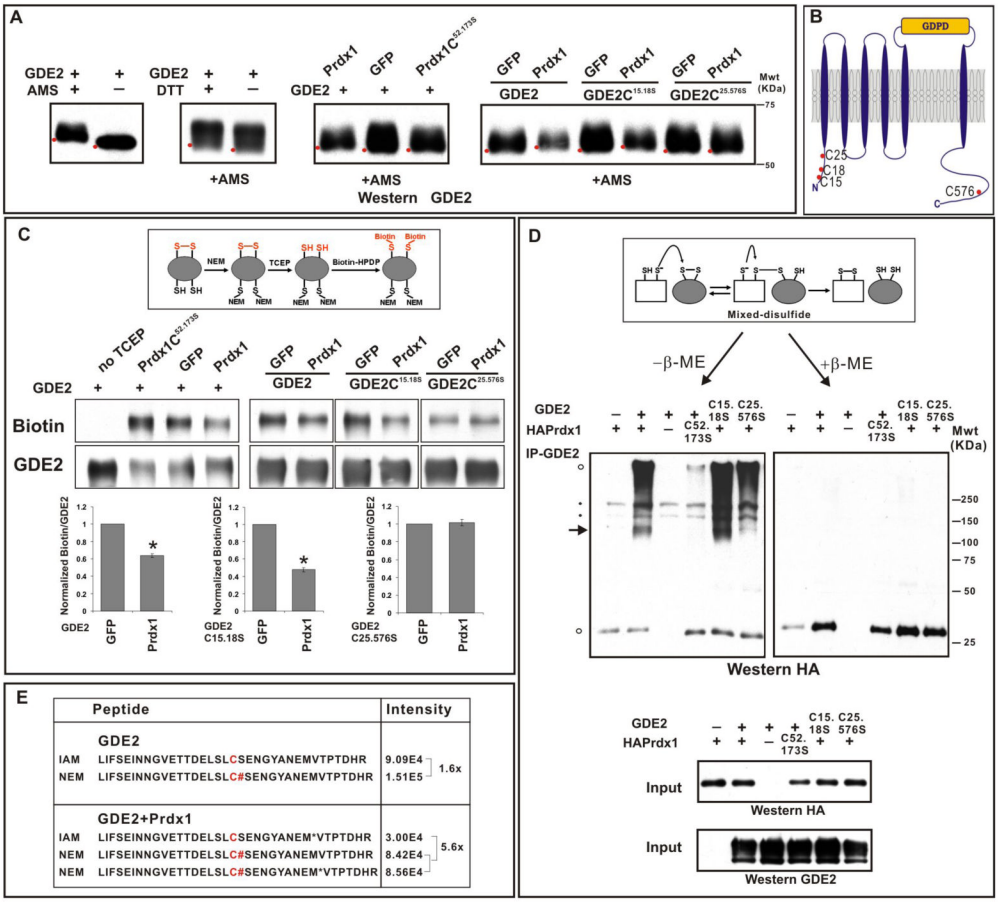

Figure 6. Prdx1 reduces an intracellular disulfide bridge in GDE2

(A) Western blots of AMS modified surface biotinylated GDE2 in transfected HEK293T cells. Red dots mark horizontal position of the bands. Similar results were obtained with total protein. Addition of DTT caused further shifts in GDE2 mobility consistent with the presence of additional disulfide bonds in GDE2. MS analysis reveals that C15 and C18 can form a disulfide bond that is insensitive to Prdx1 activity (data not shown) (B) Schematic of intracellular cysteines in GDE2, other cysteines are not marked (C) Western blots of IP-ed GDE2 detecting biotinylated GDE2 compared with GDE2. Graphs quantify the amount of biotinylated GDE2 normalized to total GDE2, mean ± s.e.m., GDE2 + GFP values are normalized to 1, GDE2 + Prdx1 *p= 6.4×10^{-18}, $GDE2C^{15.18S}$ + Prdx1 *p= 2.05×10^{-13}, $GDE2C^{25.576S}$ + Prdx1 p= 0.27; n= 7 assays; one sample student's t-test. (D) Non-reducing gels of GDE2 coIPs from transfected HEK293T cells with or without β-mercaptoethanol (β-ME). Arrow = 120–130KDa mixed-disulfide Prdx1/glycosylated GDE2 intermediate. Black circles: non-specific bands; open circles: higher order Prdx1-containing oligomers, Prdx1 monomers. The band comigrating with the Prdx1 monomer in lane 1 is not specific and forms a minor component when Prdx1 complexes interacting with GDE2 are reduced by β-ME. (E) Relative signal intensities of GDE2 C-terminal peptides containing C576 labeled with IAM (C; oxidized thiol) or NEM (C#; free thiol) in the absence or presence of Prdx1. Ratio= NEM/IAM.

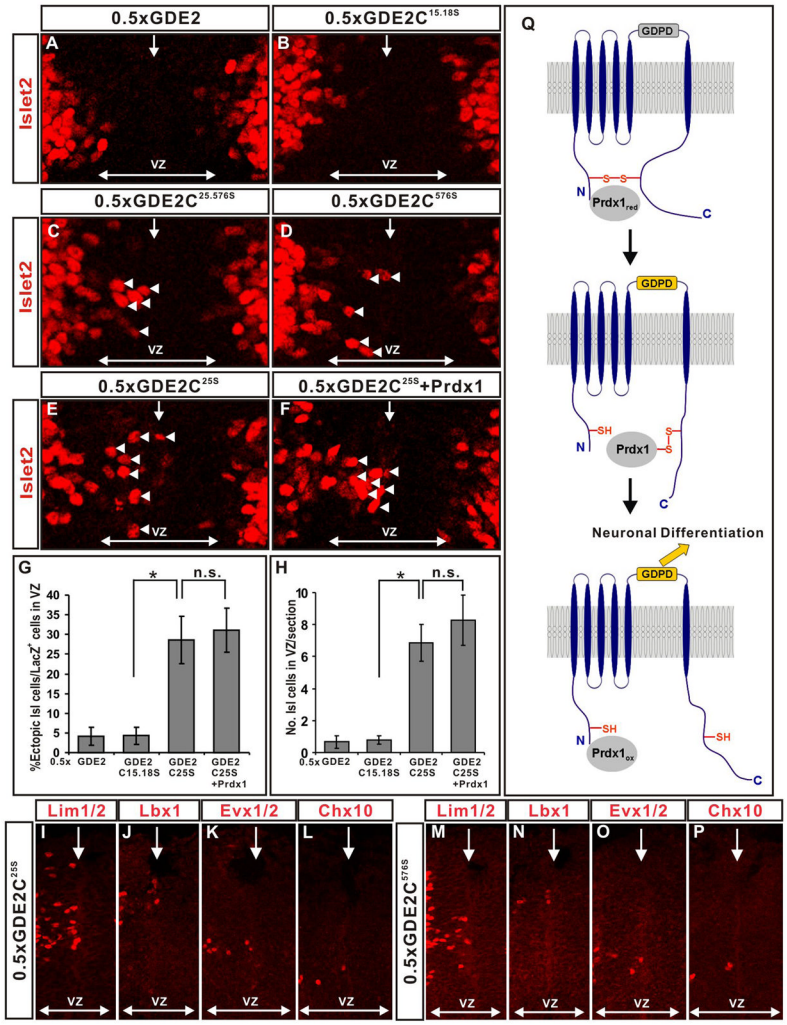

Figure 7. GDE2 variants incapable of forming the N-C disulfide bridge are more active and lose Prdx1 synergy

(A-F) Immunohistochemical analyses of ventral and dorsal (I-P) St 19–20 electroporated chick spinal cords (left). Arrowheads mark Islet2^{+} motor neurons in the ventricular zone (VZ). Midline: vertical arrow, VZ: horizontal arrow. (G) Graphs quantifying the percentage of ectopic motor neurons relative to the number of transfected cells (LacZ) and the number of ectopic motor neurons (H) in the VZ (mean ± s.e.m; * = $p<0.001$, two-tailed student's t-test, n= 7–10; n.s.= $p > 0.5$). (Q) Model for Prdx1 regulation of GDE2-dependent neuronal differentiation. Reduced forms of Prdx1 bind to the N-terminus intracellular domain of GDE2. The redox active Cys of Prdx1 forms a mixed-disulfide intermediate with GDE2. Here, C576 of GDE2 participates in a direct thiol-disulfide exchange, but C25 might be utilized instead. Reduction of the GDE2 C25-C576 disulfide bond by Prdx1 activates GDE2, promoting differentiation via extracellular GDPD activity. Prdx1 is oxidized during the reaction. The reduced form of Prdx1 may be a transient component of GDE2/Prdx1 complexes.